J. Intell. Syst. **20** (2011), 279–303
DOI 10.1515/JISYS.2011.015

Automatic Detection of Defects on Periodically Patterned Textures

Asha V., Bhajantri N. U. and Nagabhushan P.

Abstract. Defect detection is a major concern in quality control of various products in industries. This paper presents two different machine-vision based methods for detecting defects on periodically patterned textures. In the first method, input defective image is split into several blocks of size same as the size of the periodic unit of the image and chi-square histogram distances of each periodic block with respect to itself and all other periodic blocks are calculated to get a dissimilarity matrix. This dissimilarity matrix is subjected to Ward's hierarchical clustering to automatically identify defective and defect-free blocks. The second method of defect detection is based on Universal Quality Index which is a measure of loss of correlation, luminance distortion and contrast distortion between any two signals. Quality indices of a periodic block with respect to itself and all other periodic blocks are calculated to get a similarity matrix containing quality indices. Specific variances of the periodic blocks are derived from the quality index matrix through orthogonal factor model based on eigen decomposition. These variances are subjected to Ward's hierarchical clustering to automatically identify defective and defect-free blocks. Results of experiments on real fabric images with defects show that the defect detection methods based on chi-square histogram distance and universal quality index yield a success rate of 98.6% and 97.8% respectively.

Keywords. Chi-square histogram, cluster, defect, eigen decomposition, periodicity, universal quality index.

2010 Mathematics Subject Classification. 93E99, 63M10, 15A23, 62H25, 15A18, 62H30.

1 Introduction

Periodically patterned textures are often found in various applications such as ceramic tiles, wallpapers, and textile fabrics. Inspection of products is a major concern in quality control of various products in industries. Among various industries, textile industry is one of the biggest traditional industries where automated inspection will help in reducing the inspection time and increasing the production rate compared to the conventional human-vision based inspection that has the following shortfalls:

- Lack of repeatability and reproducibility of inspection results due to fatigue and subjective nature of human inspections,
- Prolonged inspection time,
- Imperfect defect detection due to complicated design in textile patterns manufactured by modern textile industries.

Presently, modern textile industries produce so many varieties in fabric design. Nevertheless, all patterned fabrics produced by the modern textile industries can be grouped into only 17 wallpaper groups which are denoted as p1, p2, p3,p3m1, p31m, p4, p4m, p4g, pm, pg, pmg, pgg, p6, p6m, cm, cmm and pmm and are said to be composed of lattices of parallelogram, rectangular, rhombic, square or hexagonal shape [1, 2]. A wallpaper group has at least one of the characteristics of translational, rotational, reflectional and glide-reflectional symmetries. Strictly speaking, p1 defines a texture with just one lattice repeating itself over the complete image such as plain and twill fabrics as shown in Figure 1(a) and (b). Among the other 16 Wallpaper groups, pmm, p2 and p4m groups are called major wallpaper groups due to the fact that the wallpaper groups other than pmm, p2 and p4m groups can be transformed into these 3 major groups through geometric transformation [3]. Examples of fabrics belonging to these major wallpaper groups are shown in Figure 1(c), (d) and (e). Inspection on patterned textures belonging to wallpaper groups other than p1 group is more complicated than that in textures belonging to p1 group due to complexity in the design, existence of numerous categories of patterns, and similarity between the defect and background [4]. As a result, most of the methods in literature depend on training stage with numerous defect-free samples for obtaining decision-boundaries or thresholds prior to defect detection. This paper basically consists of two different machine-vision based methods from [5] and [6] which can detect defects on periodically patterned textures without any training stage. These methods can detect defects from images belonging to 16 out of 17 wallpaper groups. The first method is based on chi-square measure which is considered to be a measure of dissimilarity between two histograms [7] and has been widely used in various applications such as texture and object categories classification, shape matching, shape classification and boundary detection. The metric derived from chi-square measure is taken as a discriminating factor to distinguish between defective and defect-free zones in textures. The second method is based on universal quality index which is a measure of loss of correlation, luminance distortion and contrast distortion between any two signals proposed in [8]. Defective texture zones that differ in correlation, luminance and contrast with respect to defect-free texture zones can be easily captured using the concept of universal quality index. The main contributions of these two methods can be summarized as follows:

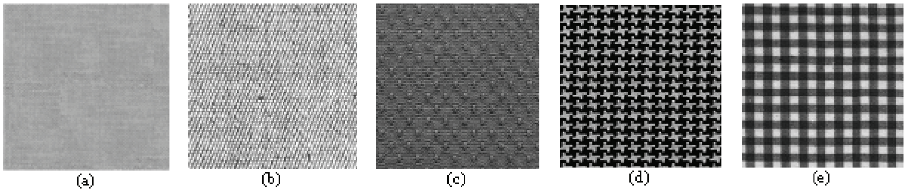

Figure 1. Fabric examples: (a) Plain fabric (p1 group); (b) Twill fabric (p1 group); (c) Dot-patterned fabric (pmm group); (d) Star-patterned fabric (p2 group); (e) Box-patterned fabric (p4m group).

- Both defect detection methods are more generic as these methods can be applied to periodic images belonging to 16 out of 17 wallpaper groups (other than p1 group images such as plain and twill fabric images).
- The methods do not require any training stage with defect-free samples for decision boundaries or thresholds unlike other methods and hence these methods do not need huge memory space for storage of defect-free samples.
- Detection of defective and defect-free periodic units is automatically carried out based on cluster analysis without human intervention.

The programs for both defect detection methods are written in Matlab-7.0 and run in a Pentium-IV Personal Computer of RAM capacity 2 GB. The organization of this paper is as follows: Section 2 gives a brief review on various methods that are available in literature for defect detection on patterned textures. Section 3 presents the defect detection method based on chi-square histogram distance along with illustration. Section 4 presents the defect detection method based on universal quality index along with illustration. Section 5 presents the results of experiments on various real fabric images with defects for both methods. Section 6 presents the performance evaluation based on precision, recall and accuracy for both methods. Section 7 has the conclusions.

2 Literature Review

Methods that are found in literature for inspection on patterned texture images include the traditional image subtraction methods [9–11], the method of golden image subtraction (GIS) [12], the method of wavelet-preprocessed golden image subtraction (WGIS) [12], the method of Direct-Thresholding (DT) based on wavelet transform [12], the Bollinger Bands method [13], the Regular Bands method [4], the Local Binary Pattern (LBP) method [14] and the motif-based methods [3, 15, 16].

Traditional image subtraction method developed by Chin and Harlow for inspection on printed circuit boards involves direct subtraction of the image under inspection with a defect-free template image [9]. Since the method involves pixel to pixel comparison, it is sensitive to noise and distortions. Khalaj et al. developed a method of inspecting patterned wafers based on periodicity estimation using gray value projection and a reference image that is constructed from the input image itself using average gray values of all repetitive units [10]. Pixel-to-pixel comparison between the input image and the reference image based on assumed threshold helps in identifying the location of defects. Xie and Guan presented a similar method wherein the building block required for constructing reference image is extracted using linear interpolation technique [11]. However, if the defect size in the image is too large, the building block constructed based on the methods suggested in [10] and [11] can never be a good estimate of the true value.

The basic GIS method involves training stage with defect-free samples and testing stage [12]. In training stage, energy of golden image subtraction defined as sum of absolute difference between the golden image (a template unit of size more than that of the periodic unit) and a histogram-equalized reference image (defect-free image) over a given window is obtained at every pixel location and thresholds are obtained from several defect-free samples. In testing stage, energies obtained from golden image and defective test images are compared with the thresholds obtained from the training stage to find the defects after filtering using median filter or Weiner filter. The method was tested with 30 defect-free and 30 defective pmm images. The detection success rates for the pmm images are 100% for defect-free images and 56.67% for defective images. The overall success rate is 78.33%. In order to overcome the sensitivity of this method to noise, the WGIS method was developed [12]. This is similar to the GIS method expect that Haar wavelet transform is applied to all images and the sub-images (in level-1 approximation) are utilized instead of original image. The overall success rate was improved to 96.7%. In the method of DT [12], Haar wavelet transform is applied on reference images and fourth level horizontal and vertical details are extracted. Lower and upper bound values of the three horizontal details in level-4 and also vertical details are extracted and their averages are calculated after filtering. Thresholds obtained using these horizontal and vertical details in training stage with defect-free images are utilized in testing stage for finding the defects in images of pmm wallpaper group. The detection success rates are 86.77% for defect-free images and 90% for defective images. The overall detection success rate is 88.3%.

The Bollinger Bands are basically measures of oversold and overbought trends in stock markets, and are calculated based on moving average and standard deviation. Ngan and Pang extended Bollinger Bands (BB) from a one-dimensional approach into a two-dimensional approach for defect detection on patterned Jacquard fabrics belonging to pmm group [13]. The application of BB for defect detection is in two stages, namely, training stage and testing stage. Upper and lower Bollinger bands are calculated for the reference images in training stage based on mean and standard deviation and the size of the repetitive unit. Thresholds obtained in the training stage are later used for detecting defects from defective images in testing stage. The method was tested on pmm, p2 and p4m wallpaper groups with 167 defect-free images and 171 defective images and the detection success rate was found to be 98.59%.

Ngan and Pang presented another approach called Regular Bands (RB) method for defect detection on patterned textures with the help of moving average and standard deviation [4]. Thresholds obtained from several histogram-equalized defect-free images during training stage were used for detecting defects on histogram-equalized defective images during testing stage. The method was tested on pmm, p2 and p4m wallpaper groups with 80 defect-free images and 86 defective images and the detection success rate was found to be 99.4%.

Fabric defect detection using modified local binary pattern (LBP) [14] involves two stages, namely, Training Stage and Defect Detection Stage. In the training stage, LBP operator is applied to an image of defect-free fabric, pixel-by-pixel, and a reference feature vector is computed. The defect-free fabric is then divided into several windows of size slightly more than that of periodic unit and LBP operator is applied to each of these windows to get a suitable threshold from the defect-free image. In the detection stage, the defective fabric is divided into several windows (as in training stage) and LBPs are obtained. Defects are then located in the fabric based on the threshold. The method was tested on pmm, p2 and p4m images and the detection success rate was found to be 96.7%.

Ngan et al [3, 15, 16] developed motif-based methods for detecting defective lattices from 16 out of 17 wallpaper groups based on energy and variance of the hand-located lattices. Minimum-maximum decision boundaries (rectangular boundaries) are obtained in energy-variance space from several defect-free test images using hand-located defect-free and defective lattices that are composed of motifs [3, 15]. Energy of moving subtraction between a motif and its circular shift matrices is derived using norm-metric measurement and variance of the energies for all motifs is obtained. By learning the distribution of these values over a number of defect-free lattices, boundary conditions for discerning defective and defect-free lattices are obtained. As the 16 wallpaper groups of patterned fabric can be transformed into three major groups, namely, pmm, p2 and p4m, the method was evaluated over these three major groups. Based on the decision boundaries obtained using 160 defect-free lattices samples, the method was tested with 140 defect-free and 113 defective samples. An overall detection success rate of 93.3% was achieved. Ngan et al. [16] later proved that instead of minimum-maximum boundaries, when ellipsoidal decision boundaries are utilized (based on the assumption that energy-variance values of defect-free lattices follow Gaussian distribution), the average detection success rate increases to 95.8%.

3 Defect Detection based on Chi-square Histogram Distance

The chi-square measure is one of the powerful measures for better discrimination between two histograms and has been widely used in various applications such as texture and object categories classification, shape matching, shape classification and boundary detection. This section presents the defect detection method based on chi-square histogram distance from [5] in detail along with illustration.

3.1 Brief Review on Chi-square Histogram Distance

In histograms of many processes, the difference between large bins is less important than the difference between small bins and should be reduced for better discrimination between two histograms. The chi-square histograms take this into account [17]. In fact, the chi-square histogram distance comes from the chi-square statistics used to test the best fit between a distribution and observed frequencies. If p and q represent first order histograms of two different images A and B of size $M \times N$, the chi-square measure between these two histograms is given by

$$\chi^2(p, q) = \frac{1}{2} \sum_{k=0}^{L-1} \frac{[p(r_k) - q(r_k)]^2}{p(r_k) + q(r_k)}. \tag{1}$$

The first order histograms are given as

$$p(r_k) = \frac{n_{A,i}}{n}, \quad q(r_k) = \frac{n_{B,i}}{n}, \quad i = 0, 1, 2, \ldots, L-1, \tag{2}$$

where $n_{A,i}$ is the number of pixels that have gray level r_k in the image A, $n_{B,i}$ is the number of pixels that have gray level r_k in the image B, n is the total number of pixels in the image A or B, and L is the total number of gray values in the image A or B. The square root of chi-square measure is a distance metric [17] which is termed here as *Chi-square Histogram Distance* χ.

3.2 Algorithm Description

There are three main assumptions in the proposed algorithm as follows:

- Test image is of at least two periodic units in horizontal direction and two in vertical direction whose dimensions are known a priori.

- Number of defective periodic units is always less than the number of defect-free periodic units.

- Test images are from imaging system oriented perpendicular to the surface of the product such as textile fabric. This assumption is due to the fact that in a defect detection system in industries such as fabric industry, the imaging system is always oriented perpendicular to the plane of fabric surface.

The main idea here is to analyze the periodic blocks from the test image for finding the defects. Hence, based on our earlier approach of analyzing patterned textures [18], four cropped images are obtained from the defective test image by cropping it from all four corners (top-left, bottom-left, top-right and bottom-right). If g is an image of size $M \times N$ with row periodicity P_r (i.e., number of columns in a periodic unit) and column periodicity P_c (i.e., number of rows in a periodic unit), then the size of cropped image g_{crop} is $M_{\text{crop}} \times N_{\text{crop}}$ where M_{crop} and N_{crop} are measured from top-left, bottom-left, top-right and bottom-right corners and are given by the following equations:

$$M_{\text{crop}} = \text{floor}(M/P_c) \times P_c \tag{3}$$

$$N_{\text{crop}} = \text{floor}(N/P_r) \times P_r. \tag{4}$$

Each cropped image is split into several periodic blocks of size $P_c \times P_r$ and the distance metrics based on chi-square measures are calculated for each periodic block with respect to itself and all other periodic blocks to get a distance matrix (dissimilarity matrix). If a cropped image has n_p number of periodic blocks, then the dissimilarity matrix is a square matrix of size $n_p \times n_p$ as given below:

$$\Psi = \begin{bmatrix} \chi_{1,1} & \chi_{1,2} & \cdots & \chi_{1,n_p-1} & \chi_{1,n_p} \\ \chi_{2,1} & \chi_{2,2} & \cdots & \chi_{2,n_p-1} & \chi_{2,n_p} \\ \vdots & \vdots & \ddots & \vdots & \vdots \\ \chi_{n_p-1,1} & \chi_{n_p-1,2} & & \chi_{n_p-1,n_p-1} & \chi_{n_p-1,n_p} \\ \chi_{n_p,1} & \chi_{n_p,2} & \cdots & \chi_{n_p,n_p-1} & \chi_{n_p,n_p} \end{bmatrix}. \tag{5}$$

Since χ of a periodic block with itself is zero and χ between i^{th} periodic block and j^{th} periodic block is same as χ between j^{th} periodic block and i^{th} periodic block, the dissimilarity matrix becomes a diagonally symmetric hollow matrix (with diagonal elements being zero) as below:

$$\Psi = \begin{bmatrix} 0 & & & & \\ \chi_{2,1} & 0 & & & \\ \vdots & \vdots & \ddots & & \\ \chi_{n_p-1,1} & \chi_{n_p-1,2} & & 0 & \\ \chi_{n_p,1} & \chi_{n_p,2} & \cdots & \chi_{n_p,n_p-1} & 0 \end{bmatrix} \tag{6}$$

It may be noted that the upper diagonal elements are not filled for the sake of simplicity. In order to extract defective and defect-free clusters from this dissimilarity matrix, Ward's hierarchical algorithm which is based on inner squared distance and minimum variance criterion [19] is utilized and a cluster tree is obtained in the form of a linkage matrix Z of size $(n_p - 1) \times 3$. The leaf nodes in the cluster hierarchy are the periodic blocks in the original data set numbered from 1 to n_p. These are the singleton clusters from which all higher clusters are built. Each newly formed cluster, corresponding to row i in Z, is assigned the index $n_p + i$. The first and second columns of the linkage matrix contain the indices of the periodic blocks that were linked in pairs to form a new cluster. This new cluster is assigned the index value $n_p + i$. There are $n_p - 1$ higher clusters corresponding to the interior nodes of the hierarchical cluster tree. The third column contains the corresponding linkage distances between the periodic blocks paired in the clusters at each row i. The last value of the linkage distance is maximum indicating that all periodic blocks are grouped into one cluster and the last but one value of the linkage distance is the next maximum corresponding to two clusters, yielding the required cut-off point at which two clusters (one cluster containing defective periodic blocks and other cluster containing defect-free periodic blocks) are formed. Upon identifying the two clusters, the number of periodic blocks in one cluster is compared with that of other and the cluster with less number of periodic blocks is assumed to be defective. Detection of defective blocks from each cropped image does not give an overview of the total defects in the input defective image. Hence, in order to get the overview of the total defects in the input image, concept of *fusion* of defects proposed in [18] is utilized that involves merging of boundaries of the defective blocks identified from each cropped image, morphological filling [20] and Canny edge detection [20]. The entire procedure for defect detection based on chi-square histogram distance is shown in the form of flow chart in Figure 2.

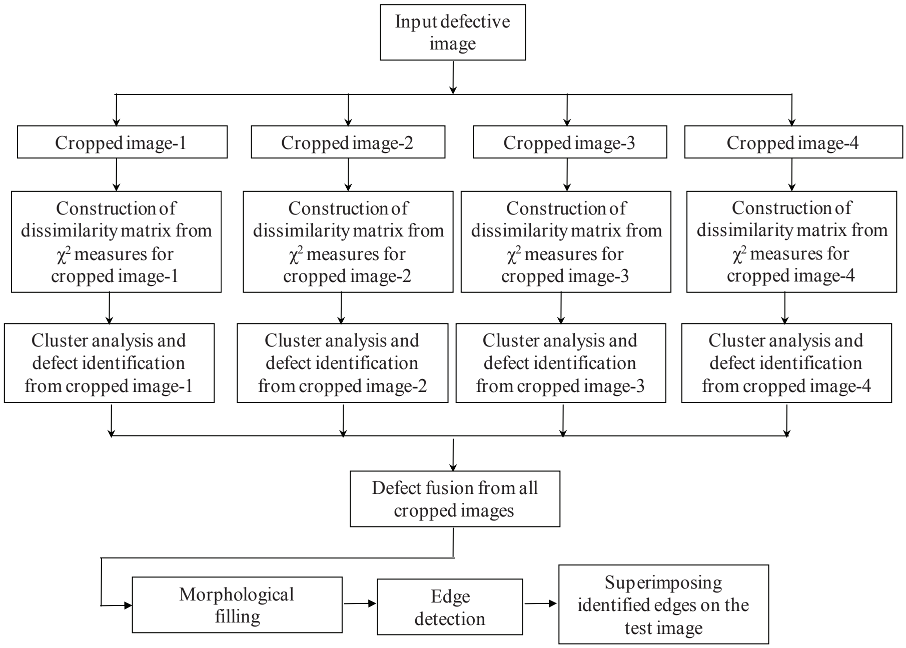

Figure 2. Defect detection scheme based on chi-square histogram distance.

3.3 Algorithm Illustration with Example

In order to illustrate the method of defect detection based on chi-square histogram distance, let us consider a defective box-patterned fabric image (pmm image) as shown in Figure 3(a). Following equations (3) and (4), four cropped images containing complete number of periodic blocks are obtained as shown in Figure 3(b)–(e) from the test image with the help of periodicities known a priori.

Each cropped image is split into several blocks of size same as the size of the periodic unit and chi-square distance metrics are calculated for each block with respect to itself and all other periodic blocks to get the dissimilarity matrix from equation (6). A typical cropped image split into several periodic blocks is shown in Figure 4(a) and the numbering sequence followed for each periodic block is shown in Figure 4(b). The dissimilarity matrices obtained from the cropped images are shown in Figure 5 in gray-scale form by scaling the matrix elements linearly in the range 0–255. It may be noted from Figure 5 that the diagonal elements in the dissimilarity matrix indicate that the periodic blocks are of zero dissimilarity with themselves and that the dissimilarity matrix is symmetric. The dissimilarity matrices are subjected to Ward's hierarchical clustering to discriminate between

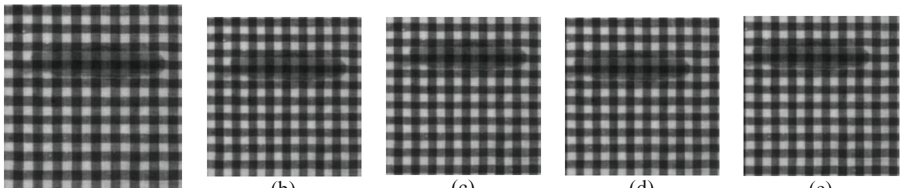

(a) (b) (c) (d) (e)

Figure 3. (a) Input defective image; (b) Cropped image obtained from top-left corner of the test image; (c) Cropped image obtained from bottom-left corner of the test image; (d) Cropped image obtained from top-right corner of the test image; (e) Cropped image obtained from bottom-right corner of the test image.

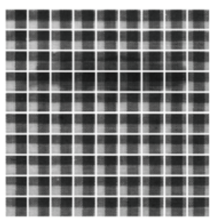

(a)

1	11	21	31	41	51	61	71	81
2	12	22	32	42	52	62	72	82
3	13	23	33	43	53	63	73	83
4	14	24	34	44	54	64	74	84
5	15	25	35	45	55	65	75	85
6	16	26	36	46	56	66	76	86
7	17	27	37	47	57	67	77	87
8	18	28	38	48	58	68	78	88
9	19	29	39	49	59	69	79	89
10	20	30	40	50	60	70	80	90

(b)

Figure 4. (a) A cropped image split into several periodic blocks; (b) Numbering sequence followed for the periodic blocks.

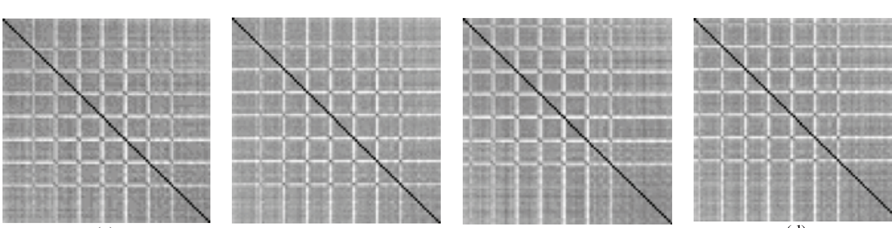

(a) (b) (c) (d)

Figure 5. Dissimilarity matrix derived from the chi-square histogram distances of cropped images obtained from (a) top-left (b) bottom-left (c) top-right and (d) bottom-right corners of the test image shown in gray-scale.

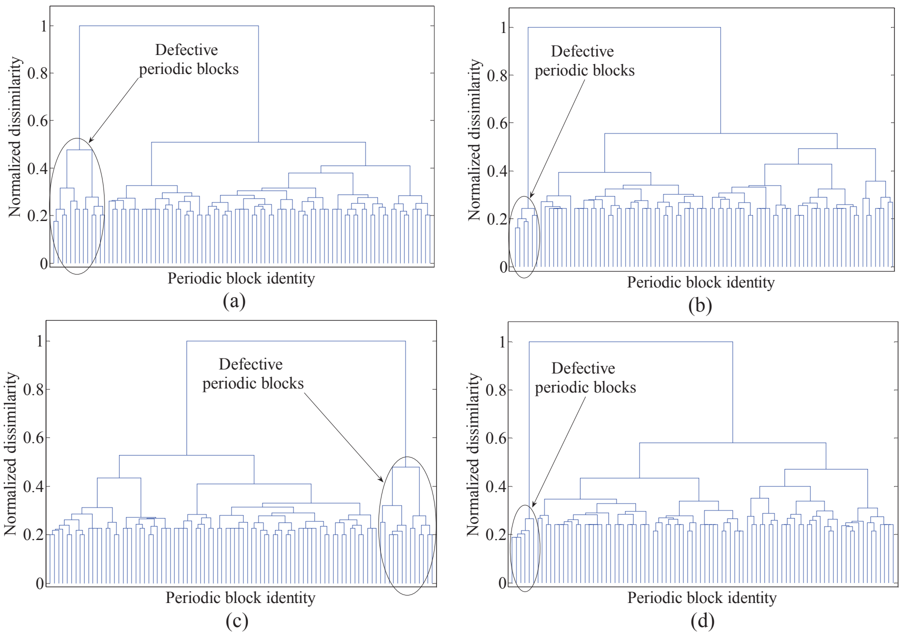

Figure 6. Dendrograms resulting from cluster analysis of chi-square dissimilarity matrix obtained from the test image by cropping from (a) top-left (b) bottom-left (c) top-right and (d) bottom-right corners. Defective blocks identified from these cropped images are (44, 64, 54, 34, 24, 74, 14, 23, 73, 33, 63, 43, and 53), (43, 63, 33, 53, 23, and 73), (44, 54, 24, 34, 64, 4, 14, 13, 63, 23, 53, 33, and 43) and (33, 53, 23, 43, 63, and 13). It may be noted that since the cropped images have more number of periodic blocks, the identities of the periodic blocks in the abscissa are not shown in order to avoid crowd and to have better clarity.

defective and defect-free blocks automatically. The resulting dendrograms after normalization indicating the two clusters are shown in Figure 6. The defective blocks thus identified from each cropped image are shown in Figure 7.

The boundaries of defective periodic blocks identified from each cropped image are shown superimposed on the original defective image in Figure 8(a) and shown separately on plain background in Figure 8(b). These zones are morphologically filled as shown in Figure 8(c) and their edges are extracted using Canny's edge operator as shown in Figure 8(d). The extracted edges are shown superimposed on original defective image in Figure 8(e). Thus, it is clear that *fusion* of defects from all 4 cropped images helps in getting an overview of total defects in the input image.

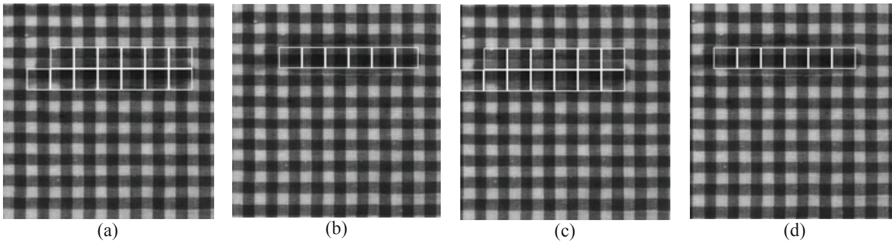

Figure 7. Defective periodic blocks identified from the cluster analysis of chi-square dissimilarity matrix derived from the cropped images obtained from (a) top-left (b) bottom-left (c) top-right and (d) bottom-right corners of the test image with their boundaries highlighted using white pixels.

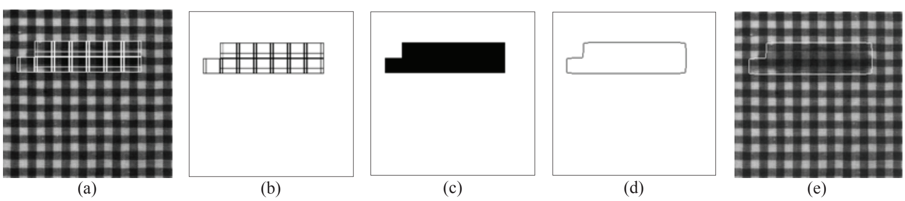

Figure 8. Illustration of defect fusion for the method based on chi-square histogram distance: (a) Boundaries of the defective blocks identified from each cropped image shown superimposed on the original defective image; (b) Boundaries of the defective blocks shown separately on plain background; (c) Result of morphological filling; (d) Canny edge detection; (e) Identified edges shown superimposed on the original defective image using white pixels.

4 Defect Detection based on Universal Quality Index

Universal Quality Index is a measure of loss of correlation, luminance distortion and contrast distortion between any two signals [8]. Defective zones of a patterned texture will differ in correlation, luminance or contrast with respect to that of defect-free zones of the texture. Hence, defective zones can be easily identified using the concept of universal quality index. This section presents the defect detection method based on universal quality index from [6] in detail along with illustration.

4.1 Brief Review on Universal Quality Index

According to Wang and Bovik [8], the universal quality index which is a measure of similarity between two signals $x = \{x_i \mid i = 1, 2, \dots N\}$ and $y = \{y_i \mid i =$

$1, 2, \ldots N\}$ is given by

$$q_{x,y} = \frac{4\sigma_{xy}\overline{x}\,\overline{y}}{(\sigma_x^2 + \sigma_y^2)\{(\overline{x})^2 + (\overline{y})^2\}} \tag{7}$$

where,

$$\overline{x} = \frac{1}{N}\sum_{i=1}^{N} x_i, \quad \overline{y} = \frac{1}{N}\sum_{i=1}^{N} y_i, \quad \sigma_{xy} = \frac{1}{N-1}\sum_{i=1}^{N}(x_i - \overline{x})(y_i - \overline{y}),$$

$$\sigma_x^2 = \frac{1}{N-1}\sum_{i=1}^{N}(x_i - \overline{x})^2, \quad \sigma_y^2 = \frac{1}{N-1}\sum_{i=1}^{N}(y_i - \overline{y})^2.$$

Equation (7) can be rearranged and written as

$$q_{x,y} = \frac{\sigma_{xy}}{\sigma_x\sigma_y} \cdot \frac{2\overline{x}\,\overline{y}}{(\overline{x})^2 + (\overline{y})^2} \cdot \frac{2\sigma_x\sigma_y}{\sigma_x^2 + \sigma_y^2}. \tag{8}$$

The first component in the equation is the correlation coefficient between the two signals that measures the degree of correlation between the two signals and its dynamic range is (−1, 1). The second component is the measure of mean luminance between the two signals whose dynamic range is (0, 1). The third component is a measure of how close the contrasts of the two signals are. Its dynamic range is also (0, 1). Thus, the quality index takes into account three factors namely, loss of correlation, luminance distortion and contrast distortion between two signals.

4.2 Algorithm Description

Similar to the previous method based on chi-square histogram distance, each cropped image is split into n_p number of periodic blocks of size $P_c \times P_r$ and quality indices of each periodic block with respect to itself and all other periodic blocks are calculated to get a similarity matrix (similar to correlation matrix) as given below:

$$Q = \begin{bmatrix} q_{1,1} & q_{1,2} & \cdots & q_{1,n_p-1} & q_{1,n_p} \\ q_{2,1} & q_{2,2} & \cdots & q_{2,n_p-1} & q_{2,n_p} \\ \vdots & \vdots & \ddots & \vdots & \vdots \\ q_{n_p-1,1} & q_{n_p-1,2} & \cdots & q_{n_p-1,n_p-1} & q_{n_p-1,n_p} \\ q_{n_p,1} & q_{n_p,2} & \cdots & q_{n_p,n_p-1} & q_{n_p,n_p} \end{bmatrix}. \tag{9}$$

For each cropped image with n_p number of periodic blocks, the size of the similarity matrix is $n_p \times n_p$. This matrix is here referred to as *quality index matrix*. Since the quality index of a periodic block with itself is *one* and the quality index between i^{th} periodic block and j^{th} periodic block is same as the quality index between j^{th} periodic block and i^{th} periodic block, the similarity matrix becomes a diagonally symmetric matrix with diagonal elements being *one* as below:

$$Q = \begin{bmatrix} 1 & & & & \\ q_{2,1} & 1 & & & \\ \vdots & \vdots & \ddots & & \\ q_{n_p-1,1} & q_{n_p-1,2} & \cdots & 1 & \\ q_{n_p,1} & q_{n_p,2} & \cdots & q_{n_p,n_p-1} & 1 \end{bmatrix}. \tag{10}$$

It may be noted that since the matrix is symmetric about the diagonal, the upper diagonal elements are not filled for the sake of simplicity. This similarity matrix does not yield directly any useful measure to discriminate between defective and defect-free periodic blocks as the matrix yields joint or pair-wise information. Hence, in order to extract useful measure for creating a feature space for cluster analysis and thereby to identify defective and defect-free clusters, the concept of *Orthogonal Factor Model* is utilized. According to the orthogonal factor model, an observable random vector X with p components and mean vector μ can be expressed as a linearly dependent function of a few random variables $F_1, F_2, \ldots, F_m$, called common factors, and p additional sources of variation $\varepsilon_1, \varepsilon_2, \ldots, \varepsilon_p$ called errors or specific factors and can be given as [21]

$$\begin{aligned} X_1 - \mu_1 &= l_{11}F_1 + l_{12}F_2 + \cdots + l_{1m}F_m + \varepsilon_1, \\ X_2 - \mu_2 &= l_{21}F_1 + l_{22}F_2 + \cdots + l_{2m}F_m + \varepsilon_2, \\ &\vdots \\ X_p - \mu_p &= l_{p1}F_1 + l_{p2}F_2 + \cdots + l_{pm}F_m + \varepsilon_p, \end{aligned} \tag{11}$$

where the coefficient l_{ij} is called the loading of i^{th} variable on j^{th} factor. All these coefficients form the loading matrix L of size $p \times m$. In matrix notation, equation (11) can be written as

$$X - \mu = LF + \varepsilon, \tag{12}$$

where

$$X = \begin{pmatrix} X_1 \\ X_2 \\ \vdots \\ X_p \end{pmatrix}, \quad \mu = \begin{pmatrix} \mu_1 \\ \mu_2 \\ \vdots \\ \mu_p \end{pmatrix}, \quad L = \begin{pmatrix} l_{11} & l_{12} & \cdots & l_{1m} \\ l_{21} & l_{22} & \cdots & l_{2m} \\ \vdots & \vdots & \ddots & \vdots \\ l_{p1} & l_{p2} & \cdots & l_{pm} \end{pmatrix},$$

$$F = \begin{pmatrix} F_1 \\ F_2 \\ \vdots \\ F_p \end{pmatrix}, \quad \text{and} \quad \varepsilon = \begin{pmatrix} \varepsilon_1 \\ \varepsilon_2 \\ \vdots \\ \varepsilon_p \end{pmatrix}.$$

In terms of correlation matrix of X, equation (12) can be expressed as

$$\rho = \mathrm{Cor}(X) = LL^T + \Psi, \tag{13}$$

where ρ is the correlation matrix of X, L^T is the transpose of factor loading matrix of size $m \times p$, and Ψ is the diagonal matrix containing specific variances as the diagonal elements. The portion of correlation of i^{th} variable contributed by the m common factors is called the i^{th} communality and that due to specific factor is called uniqueness or specific variance. Representing the i^{th} communality by h_{i}^2, equation (13) can be written as

$$\rho_{ii} = h_i^2 + \psi_i, \quad i = 1, 2, \ldots, p, \tag{14}$$

where $h_i^2 = l_{i1}^2 + l_{i2}^2 + \cdots + l_{im}^2$. The i^{th} communality is the sum of squares of the loadings of the i^{th} variable on the m common factors. If the off-diagonal elements in the correlation matrix ρ are zero, the variables are not correlated and the factor analysis will not be useful. Under such circumstances, the specific factors are very much useful. In fact, the prime motive of the factor analysis is to estimate few significant common factors. Solving equation (13) involves estimation of the loading matrix L and the specific variance matrix Ψ from the correlation matrix ρ using techniques such as Principal Component Analysis (PCA) [21]. According to the method of PCA, the correlation matrix ρ can be written in terms of eigenvalue-eigenvector pairs (λ_i, e_i) through eigen decomposition. Eigen decomposition or spectral decomposition is the factorization of a square matrix into a canonical form, where the square matrix is represented in terms of its eigenvalues and eigenvectors [21]. Now, based on eigen decomposition, the symmetric matrix ρ can be factorized as $\rho = E\Lambda E^{\mathrm{T}}$, where, E is the orthogonal square matrix of size $p \times p$ whose i^{th} column is the eigenvector e_i of E and Λ is the diagonal matrix whose diagonal elements are the corresponding eigenvalues, i.e., $\Lambda_{ii} = \lambda_i$, such that $\lambda_1 \geq \lambda_2 \geq \lambda_3 \geq \cdots \geq \lambda_p \geq 0$. In terms of components, ρ can be expressed as

$$\rho = \lambda_1 e_1 e_1^{'} + \lambda_2 e_2 e_2^{'} + \cdots + \lambda_p e_p e_p^{'}. \tag{15}$$

In vectorial form, ρ can be expressed as

$$\rho = \left[\sqrt{\lambda_1} e_1 \; \sqrt{\lambda_2} e_2 \; \cdots \sqrt{\lambda_p} e_p \right] \begin{bmatrix} \sqrt{\lambda_1} e_1^{'} \\ \sqrt{\lambda_2} e_2^{'} \\ \vdots \\ \sqrt{\lambda_p} e_p^{'} \end{bmatrix}. \tag{16}$$

If a factor model has as many factors as the variables ($m = p$), then $\Psi_i = 0$ for all i and $\rho = LL^T$. This does not allow any variation in the specific factor and hence the model is not useful. However, models that explain the correlation structure in terms of few common factors can be preferred for extraction of useful feature (specific variance) in certain applications. When m eigenvalues are enough for approximating the correlation matrix, the approximate representation of equation (16) with m factors can be given as

$$\rho \approx \begin{bmatrix} \sqrt{\lambda_1} e_1 & \sqrt{\lambda_2} e_2 & \cdots & \sqrt{\lambda_m} e_m \end{bmatrix} \begin{bmatrix} \sqrt{\lambda_1} e_1^{'} \\ \sqrt{\lambda_2} e_2^{'} \\ \vdots \\ \sqrt{\lambda_m} e_m^{'} \end{bmatrix}. \tag{17}$$

Allowing for specific factors, for a m-factor model with $m < p$, the approximation becomes

$$\rho = \left[\sqrt{\lambda_1} e_1 \; \sqrt{\lambda_2} e_2 \; \cdots \; \sqrt{\lambda_m} e_m \right] \begin{bmatrix} \sqrt{\lambda_1} e_1^{'} \\ \sqrt{\lambda_2} e_2^{'} \\ \vdots \\ \sqrt{\lambda_m} e_m^{'} \end{bmatrix} + \begin{bmatrix} \psi_1 & 0 & \ldots & 0 \\ 0 & \psi_1 & \cdots & 0 \\ \vdots & \vdots & \ddots & \vdots \\ 0 & 0 & 0 & \psi_p \end{bmatrix}. \tag{18}$$

Since the quality index matrix is very similar to the correlation matrix, ρ can be replaced with the quality index matrix Q in equation (18) and the specific variances estimated using m factor model can be used as a feature space in clustering algorithm to form two groups, namely, defective and defect-free clusters. In order

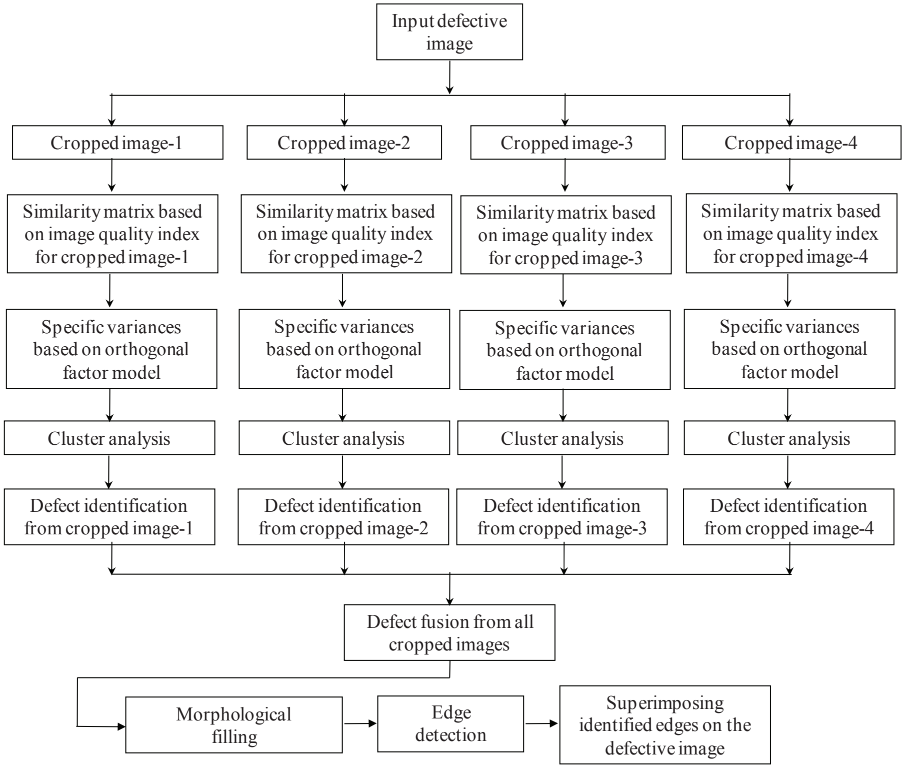

Figure 9. Defect detection scheme based on universal quality index.

to extract defective and defect-free clusters from these specific variances, Ward's hierarchical algorithm is utilized, followed by defect-fusion, morphological filling and edge-detection similar to the previous method based on chi-square histogram distance. The entire procedure for defect detection based on universal quality index is shown in the form of flow chart in Figure 9.

4.3 Algorithm Illustration with Example

In order to illustrate the method of defect detection based on universal quality index, the defective box-patterned fabric image (pmm image) shown in Figure 2(a) is considered here also. Quality indices are calculated for each block with respect to itself and all other periodic blocks and quality index matrix (similar to similarity matrix) is obtained following equation (10) for each cropped image (Figure 2(b)–(e)). The quality index matrices thus obtained are shown in Figure 10 in gray-scale form by scaling the matrix elements linearly in the range 0-255.

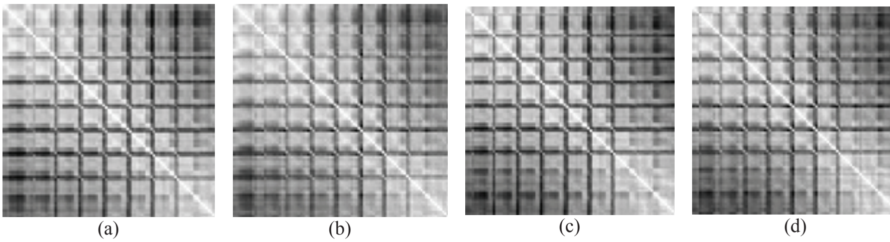

Figure 10. Quality index matrix derived from the quality indices for the cropped image obtained from (a) top-left (b) bottom-left (c) top-right and (d) bottom-right corners of the test image shown in gray-scale.

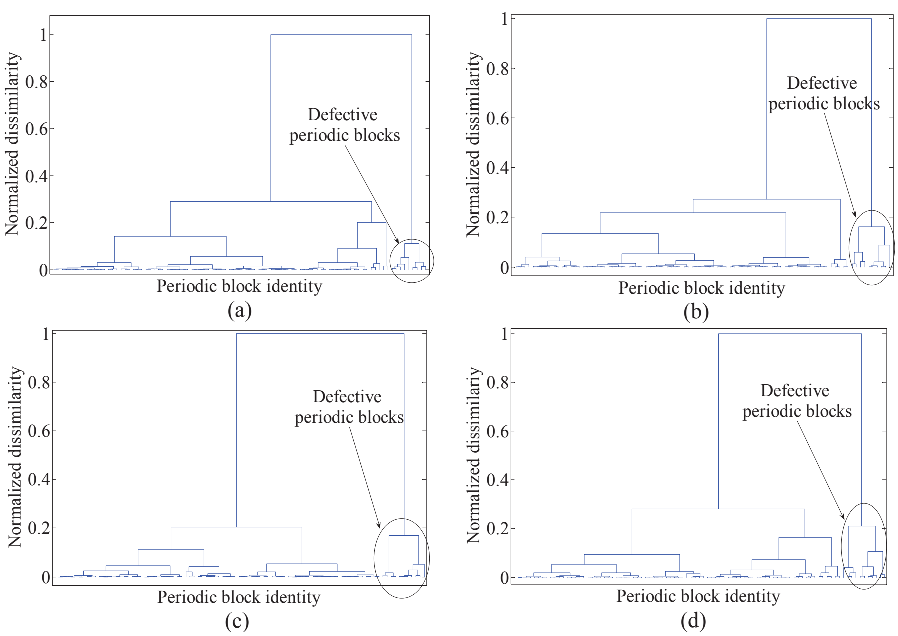

Figure 11. Dendrogram resulting from cluster analysis of specific variances obtained from the quality index matrix for the image cropped from (a) top-left (b) bottom-left (c) top-right and (d) bottom-right corners. Defective blocks identified from these cropped images are (23, 64, 63, 44, 34, 33, 43, 53, and 54), (23, 73, 34, 44, 33, 53, 63, 44, 64, and 54), (13, 34, 24, 64, 23, 43, 44, 54, 33, 53, and 63) and (13, 24, 34, 64, 23, 63, 33, 53, 43, 44, and 54). It may be noted that since the cropped images have more number of periodic blocks, the identities of the periodic blocks in the abscissa are not shown in order to avoid crowd and to have better clarity.

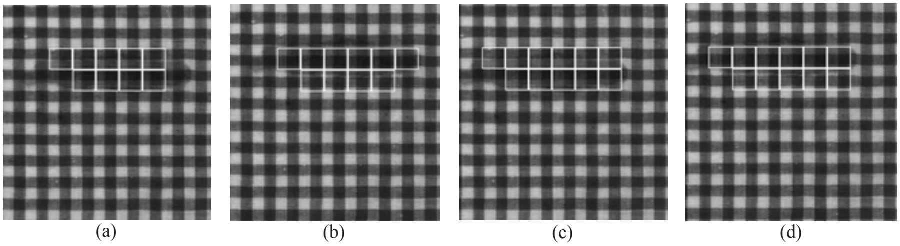

Figure 12. Defective blocks identified from the image cropped from (a) top-left (b) bottom-left (c) top-right and (d) bottom-right corners of the input image. Boundaries of the defective periodic blocks are highlighted with white pixels.

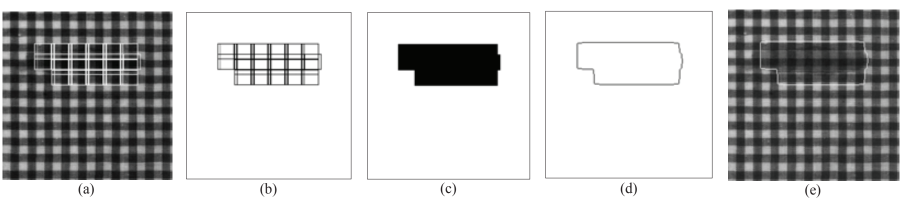

Figure 13. Illustration of defect fusion for the method based on universal quality index: (a) Boundaries of the defective blocks identified from each cropped image shown superimposed on the original defective image; (b) Boundaries of the defective blocks shown separately on plain background; (c) Result of morphological filling; (d) Canny edge detection; (e) Identified edges shown superimposed on the original defective image using white pixels.

It may be noted from Figure 10 that the diagonal elements with gray value 255 in the quality index matrix indicate that the periodic blocks are of highest correlation with themselves and that the quality index matrix is symmetric. The gray scale representation clearly indicates that locations of dark pixels correspond to the defective periodic blocks having very high dissimilarity with respect to other periodic blocks. The quality index matrix from each cropped image is subjected to orthogonal factor analysis based on eigen decomposition using two-factor model to find the specific variances. The normalized dendrograms resulting from cluster analysis of specific variances obtained from the similarity matrices of quality indices are shown in Figure 11 along with the defective periodic blocks. Boundaries of the defective periodic blocks thus identified from each cropped image are highlighted using white pixels and shown in Figure 12.

Boundaries of the defective periodic blocks identified from each cropped image are shown superimposed on the original image in Figure 13(a) and separately on a plain background in Figure 13(b). Figure 13(c) shows the result of morphological filling and Figure 13(d) shows the edges of the total defects shown separately on plain background after Canny edge detection. Figure 13(e) shows the extracted edges superimposed on the original defective image, indicating an overview of the total defects on the original image itself.

5 Experiments on Real Fabric Images with Defects

Defective fabric images belonging to three major wallpaper groups (pmm, p2 and p4m groups) are tested using both defect detection methods. As far as defect detection based on lattice concept is concerned, reason behind choosing pmm, p2, and p4m wallpaper groups is that all other wallpaper groups can be transformed into these 3 wallpaper groups through geometric transformations [3]. However, since both defect detection methods need only horizontal and vertical periodicities (row and column periodicities), there is no need for geometric transformation of wallpaper groups other than pmm, p2 and p4m into pmm, p2 and p4m groups. Figure 14 shows the defective fabric images of pmm, p2 and p4m wallpaper groups along with the defect detection results for both methods.

6 Performance Evaluation of the Defect Detection Methods

In order to evaluate the performance of both defect detection methods, performance parameters, namely, precision, recall and accuracy [22], [23] are all calculated in terms of true positive (TP), true negative (TN), false positive (FP), and false negative (FN), where true positive is defined as the number of defective periodic blocks identified as defective, true negative is defined as the number of defect-free periodic blocks identified as defect-free, false positive is defined as the number of defect-free periodic blocks identified as defective and false negative is defined as the number of defective periodic blocks identified as defect-free. Precision is defined as the number of periodic blocks correctly labeled as belonging to the positive class divided by the total number of periodic blocks labeled as belonging to the positive class and is calculated as $\mathrm{TP}/(\mathrm{TP}+\mathrm{FP})$. Recall is defined as the number of true positives divided by the sum of true positives and false negatives that are periodic blocks not labeled as belonging to the positive class but should have been and is calculated as $\mathrm{TP}/(\mathrm{TP}+\mathrm{FN})$. Accuracy is the measure of success rate that considers detection rates of both defective and defect-free periodic blocks and is calculated as $(\mathrm{TP}+\mathrm{TN})/(\mathrm{TP}+\mathrm{TN}+\mathrm{FP}+\mathrm{FN})$. Though the number of periodic blocks taken from a defective input image is same for all of its cropped images, the number of defective periodic blocks identified does not need to be

#1

#2

#3

#4

#5

#6

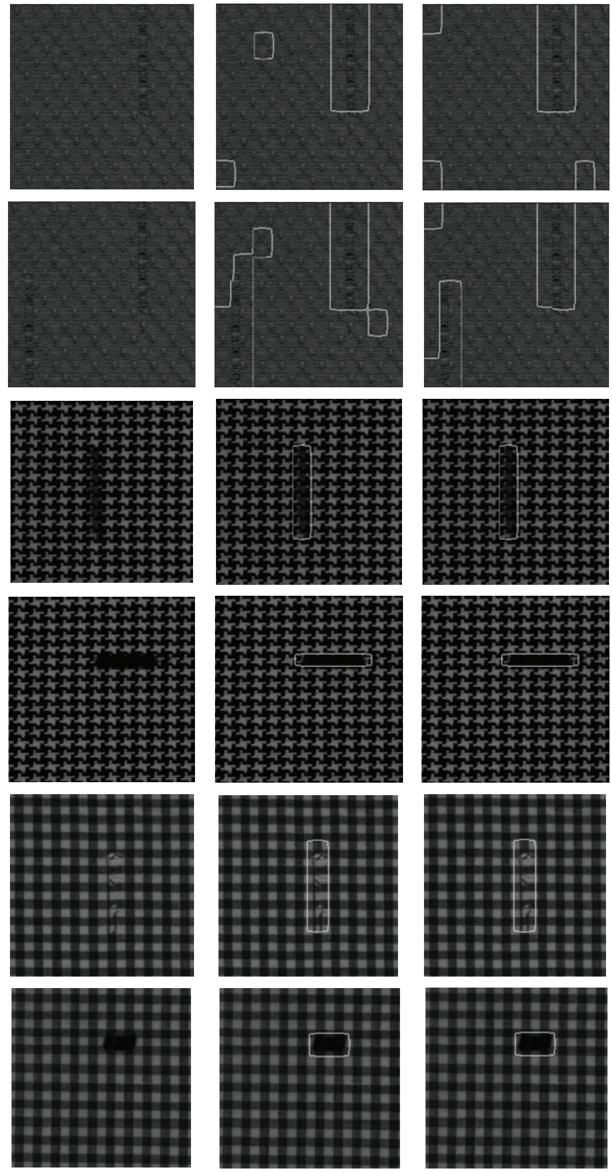

Figure 14. Final result of defect detection on sample defective fabric images: First column shows the defective fabrics; Second column shows the defect detection result based on chi-square histogram distance; Third column shows the defect detection result based on universal quality index; First and second rows indicate defective pmm images; Third and fourth rows indicate defective p2 images; Fifth and sixth rows indicate defective p4m images.

Test image	Wallpaper group	Method based on chi-square histogram			Method based on universal quality index		
		Precision (%)	Recall (%)	Accuracy (%)	Precision (%)	Recall (%)	Accuracy (%)
#1	pmm	94.4	100	99.2	86.4	100	97.6
#2	pmm	95.8	100	96.4	98.4	100	94.8
#3	p2	100	100	100	100	100	100
#4	p2	100	100	100	100	100	100
#5	p4m	100	91.7	99.4	100	91.7	99.4
#6	p4m	100	100	100	100	100	100
Demo image	p4m	100	68.0	95.3	100	74.8	96.1
	Average	98.6	94.2	98.6	97.8	95.2	98.3

Table 1. Summary of performance parameters for all defective images for both methods.

same for all cropped images. This is because the contribution of defect in each periodic block may differ for different cropped images.

Performance parameters averaged over all four cropped images for each defective image are given in Table 1 for pmm, p2 and p4m images for both methods (based on total number of periodic samples – 504, 660 and 1080 for pmm, p2 and p4m wallpaper groups respectively). The average success rates for all 3 major wallpaper groups in the unsupervised methods of defect detection based on chi-square histogram distance and universal quality index (without any training stage) are 98.6% and 97.8% respectively. The success rates obtained in these two methods are at par with the results of methods involving training stage with numerous defect-free samples, namely, Bollinger Bands method [13], Regular Bands method [4], LBP-based method [14], motif-based method with minimum-maximum decision boundaries [15], and motif-based method with ellipsoidal decision boundaries [16] which are 98.59%, 99.4%, 96.7%, 93.3%, and 95.8% respectively. It may be noted that relatively less recall rates in the proposed method indicate that there are few false negatives identified by the proposed method. However, since the proposed method yields high precision and accuracy, the proposed method can contribute to automatic defect detection in fabric industries.

7 Conclusions

Experiments on real fabric images of 3 major wallpaper groups with defects show that both chi-square histogram distance and universal quality index are very effective in indentifying fabric defects. Absence of training stage with defect-free samples for decision-boundaries or thresholds, unsupervised method of identifying defects using cluster analysis, and high success rates are the novelties of the proposed methods. Thus, it can be concluded that the defect detection methods based on chi-square histogram distance and universal quality index can contribute to the development of automatic defect detection scheme in fabric industries.

Acknowledgments. The authors would like to thank Dr. Henry Y. T. Ngan, Research Associate of Industrial Automation Research Laboratory, Department of Electrical and Electronic Engineering, The University of Hong Kong, for providing the database of patterned fabrics.

Bibliography

[1] D. Schattschneider, The Plane Symmetry Groups: Their Recognition and Notation, *Am. Math. Monthly* **85** (1978), 439–450.

[2] H. S. M. Coxeter and W. O. J. Moser, *Generators and Relations for Discrete Groups*, Fourth Edition, Springer–Verlag, New York, 1980.

[3] H. Y. T. Ngan, G. H. K. Pang and N. H. C. Yung, Performance Evaluation for Motif-Based Patterned Texture Defect Detection, *IEEE Trans. on Autom. Sci. and Eng*. **7** (1) (2010), 58–72.

[4] H. Y. T. Ngan and G. H. K. Pang, Regularity Analysis for Patterned Texture Inspection, *IEEE Trans. on Autom. Sci. and Eng*. **6** (1) (2009), 131–144.

[5] V. Asha, N. U. Bhajantri and P. Nagabhushan, Automatic Detection of Texture Defects using Texture-Periodicity and Chi-square Histogram Distance, to appear in: *Proc. of IICAI-2011*, to be held at Tumkur, India, during 14–16 December 2011.

[6] V. Asha, P. Nagabhushan and N. U. Bhajantri, Unsupervised Detection of Texture Defects using Texture-Periodicity and Universal Quality Index, to appear in: *Proc. of IICAI-2011*, to be held at Tumkur, India, during 14–16 December 2011.

[7] T. Leung and J. Malik, Representing and Recognizing the Visual Appearance of Materials using Three-dimensional Textons, *Int. J. of Comp. Vision* **43** (1) (2001), 29–44.

[8] Z. Wang and A. C. Bowik, A Universal Image Quality Index, *IEEE Signal Process. Lett*. **9** (2002), 81–84.

[9] R. T. Chin and C. A. Harlow, Automated visual inspection: A survey, *IEEE Trans. on Pattern Anal. and Mach. Intel*. **4** (6) (1982), 557–573.

[10] B. H. Khalaj and T. Kailath, Patterned wafer inspection by high resolution spectral estimation techniques, *Mach. Vision and Appl*. **7** (1994), 178–185.

[11] P. Xie and S. U. Guan, A golden-template self-generating method for patterned wafer inspection, *Mach. Vision and Appl*. **12** (2000), 149–156.

[12] H. Y. T. Ngan, G. K. H. Pang, S. P. Yung and M. K. Ng, Wavelet based methods on patterned fabric defect detection, *Pattern Recognit*. **38** (4) (2005), 559–576.

[13] H. Y. T. Ngan and G. H. K. Pang, Novel method for patterned fabric inspection using Bollinger bands, *Opt. Eng*. **45** (8) (2006), 1–15.

[14] F. Tajeripour, E. Kabir and A. Sheikhi, Fabric Defect Detection Using Modified Local Binary Patterns, in: *Proc. of the Int. Conf. on Comput. Intel. and Multimed. Appl*., pp. 261–267, 2007.

[15] H. Y. T. Ngan, G. H. K. Pang and N. H. C. Yung, Motif-based defect detection for patterned fabric, *Pattern Recognit*. **41** (2008), 1878–1894.

[16] H. Y. T. Ngan, G. H. K. Pang and N. H. C. Yung, Ellipsoidal decision regions for motif-based patterned fabric defect detection, *Pattern Recognit*. **43** (2010), 2132–2144.

[17] O. Pele and M. Werman, The Quadratic-Chi Histogram Distance Family, in: K. Daniilidis, P. Maragos, N. Paragios (Eds.): *ECCV* 2010, Part II, Lecture Notes in Computer Science 6312, pp. 749–762, Springer–Verlag, Berlin Heidelberg, 2010.

[18] V. Asha, N. U. Bhajantri and P. Nagabhushan, Automatic Detection of Texture Defects using Texture-Periodicity and Gabor Wavelets, in: K. R. Venugopal and L. M. Patnaik (Eds.): *ICIP* 2011, Communication and Computer Information Series (CCIS) 157, pp. 548–553, Springer–Verlag, Berlin Heidelberg, 2011.

[19] S. Theodoridis and K. Koutroumbas, *Pattern Recognition*, Fourth Edition. Academic Press, CA, 2009.

[20] R. C. Gonzalez and R. E. Woods, *Digital Image Processing*, Pearson Prentice Hall, New Delhi, 2008.

[21] R. A. Johnson and D. W. Wichern, *Applied Multivariate Statistical Analysis*, Fifth Edition, PHI Learning Private Limited, New Delhi, 2009.

[22] T. Fawcett, An introduction to ROC analysis, *Pattern Recognit. Lett*. **27** (2006), 861–874, 2006.

[23] C. D. Brown and H. T. Davis, Receiver operating characteristics curves and related decision measures: A tutorial, *Chemom. and Intell. Lab. Syst.* **80** (2006), 24–38.

Received June 1, 2011.

Author information

Asha V., New Horizon College of Engineering, Bangalore, Karnataka;
(Research Scholar, JSS Research Foundation, SJCE Campus, University of Mysore, Mysore, Karnataka), India.
E-mail: `v_asha@live.com`

Bhajantri N. U., Govt. Engineering College, Chamarajanagar, Mysore District, Karnataka, India.
E-mail: `bhajan3nu@gmail.com`

Nagabhushan P., University of Mysore, Mysore, Karnataka, India.
E-mail: `pnagabhushan@hotmail.com`